Nonadiabatic holonomic quantum computation using Rydberg blockade

Yi-Hao Kang,[1,2] Ye-Hong Chen,[1,2] Zhi-Cheng Shi,[1,2] Bi-Hua Huang,[1,2] Jie Song,[3] and Yan Xia[1,2,*]

[1]*Department of Physics, Fuzhou University, Fuzhou 350116, China*

[2]*Fujian Key Laboratory of Quantum Information and Quantum Optics (Fuzhou University), Fuzhou 350116, China*

[3]*Department of Physics, Harbin Institute of Technology, Harbin 150001, China*

(Received 5 December 2017; published 23 April 2018)

In this paper, we propose a scheme for realizing nonadiabatic holonomic computation assisted by two atoms and the shortcuts to adiabaticity (STA). The blockade effect induced by strong Rydberg-mediated interaction between two Rydberg atoms provides us the possibility to simplify the dynamics of the system, and the STA helps us design pulses for implementing the holonomic computation with high fidelity. Numerical simulations show the scheme is noise immune and decoherence resistant. Therefore, the current scheme may provide some useful perspectives for realizing nonadiabatic holonomic computation.

DOI: 10.1103/PhysRevA.97.042336

I. INTRODUCTION

Quantum computation has attracted many interests in recent years [1–9]. The great capability of quantum computation has been shown in the applications of quantum algorithms [10–12], quantum parallelism [13–16], and so on. This makes quantum computation a superior to solve many practical problems, such as factoring, search problems, etc. When implementing quantum computation, errors play troublesome roles, which brings challenges in constructing a real quantum computer [17]. In 1999, by taking the advantages of the geometric phase [18,19] and quantum holonomy [20,21], adiabatic holonomic quantum computation has been proposed [22] and subsequently demonstrated to hold good fault tolerance with respect to certain types of errors in the control processes [23–25]. Since then, many schemes [26–37] to realize the robust adiabatic holonomic quantum computation have been put forward with superconducting qubits [31], trapped ions [32], and quantum dots [37], etc.

However, when a system undergoes an adiabatic evolution, completing an adiabatic holonomic quantum computation usually takes a long time. To shorten the evolution time while retaining all the robustness of the adiabatic holonomic quantum computation, the concept of nonadiabatic holonomic quantum computation has been proposed [38,39]. Consider an N-dimensional quantum system governed by a Hamiltonian $H(t)$ and an L-dimensional time-dependent subspace $\mathcal{S}(t)$ spanned by a set of orthonormal basis vectors $\{|\phi_l(t)\rangle\}_1^L$ with $|\phi_l(t)\rangle$ being the solution of the Schrödinger equation $i|\dot{\phi}_l(t)\rangle = H(t)|\phi_l(t)\rangle$. It has been indicated in the scheme [38] that, if the system is initial in the subspace $\mathcal{S}(0)$, after the evolution time T, the evolution operator $U(T)$ is a holonomy matrix acting on $\mathcal{S}(0)$ when $\{|\phi_l(t)\rangle\}$ satisfy the following conditions:

$$\text{(i)}\ \sum_{l=0}^{L}|\phi_l(T)\rangle\langle\phi_l(T)| = \sum_{l=0}^{L}|\phi_l(0)\rangle\langle\phi_l(0)|, \qquad (1)$$

$$\text{(ii)}\ \langle\phi_l(t)|H(t)|\phi_{l'}(t)\rangle = 0,\ \ (l,l' = 1,2,\ldots,L). \qquad (2)$$

Here, Eq. (1) is the condition for cyclic evolution, and Eq. (2) is the holonomic condition.

To data, many fast and noise-resistant quantum computation schemes [40–54] have been presented for nuclear magnetic resonance systems [40,41], nitrogen-vacancy centers systems [42,43], superconducting systems [44–48], and some other quantum systems [49–54] by designing quantum evolutions to fulfill the holonomic conditions. Among these works about the holonomic quantum computation [40–54], schemes [43,44,48] have shown many interesting results by using the technique of shortcuts to adiabaticity (STA) [55–96]. For example, Liu *et al.* [44] have achieved holonomic quantum computation in atom-cavity coupled system by using the dressed-state based STA method [76]. Moreover, Zhang *et al.* [48] have realized fast holonomic quantum computation with the transitionless quantum driving method [55–58] of the STA. With great developments in the past few years, the STA, originally aiming at optimizing the control of a system based on a known adiabatic process, has now become a technique to drive general transitions regardless of whether the initial and final states can be adiabatically connected [96]. By merging with "inverse engineering" methods [97–102] and the optimal control methods [103–106], the STA has outranged the original aim in many applications in practice, and can now help us nonadiabatically realize arbitrary transitions or unitary transformations without referenced adiabatic processes by means of many powerful tools, such as Lewis-Riesenfeld invariant theory [58–60], Lie algebra [64,65], and so forth. Therefore, the STA might be a wonderful choice to design nonadiabatic control fields for the holonomic quantum computation in different physical systems.

On the other hand, the recent researches [107–115] on the highly excited neutral atoms have showed that atoms with long-lived Rydberg states are very promising candidates for quantum information processing. Since they provide strongly interatomic interactions that we demand in different quantum information tasks. When Rydberg-mediated interaction between two Rydberg atoms is much stronger than the intensities

*xia-208@163.com

of the driving laser pulses on atoms, the Rydberg blockade phenomenon would arise and prevent the simultaneous excitations of neighboring Rydberg atoms [116–118]. The regime of the Rydberg blockade can be used in simplifying the dynamics of the system, thus we can analytically investigate the evolution of the system based on a simplified Hamiltonian. In addition, the Rydberg states of atoms are quite stable [118,119] with small decays. Thus, when using the regime of the Rydberg blockade in quantum information tasks, the unitary evolution of the system can be protected from the decay to a certain extent.

In this paper, inspired by the interesting concept of nonadiabatic holomic quantum computation, the advantages of the STA, and the promising applications of the Rydberg blockade, we propose a scheme for realizing nonadiabatic holonomic computation with the help of two atoms and the STA. The blockade of the Rydberg atoms allows us to simplify the dynamics of the system and derive an effective Hamiltonian. By analyzing the effective Hamiltonian, we exploit the STA to design the pulses, which drive the system to complete nonadiabatic holomic two-qubit logical gates of two atoms with high fidelities. Numerical simulations indicate the current scheme is insensitive to two typical types of noise, the random noise of pulse amplitudes and the additive white Gaussian noise. Moreover, good robustness against the decoherence is also shown in the numerical simulations. Therefore, the scheme may offer some useful perspectives to the robust nonadiabatic holomic computations.

The article is organized as follows. In Sec. II A, we introduce the physical model for implementing nonadiabatic holonomic two-qubit logical gates with atoms and give the effective Hamiltonian of the system. In Sec. II B, we design the pulses driving the system to complete high-fidelity nonadiabatic holonomic two-qubit logical gates via STA. In Sec. III, numerical simulations are performed to examine the robustness of the scheme against noise and decoherence. Discussions and the conclusions are given in Sec. IV.

II. NONADIABATIC HOLONOMIC TWO-QUBIT LOGICAL GATES

A. Physical model and effective Hamiltonian

The setup for implementing nonadiabatic holonomic two-qubit logical gates is shown in Fig. 1. As shown in Fig. 1, there are two atoms a and b. Atom a (b) has two ground states $|g\rangle_{a(b)}$ and $|f\rangle_{a(b)}$, an intermediate state $|e\rangle_{a(b)}$ and a Rydberg state $|r\rangle_{a(b)}$. We consider that transition $|g(f)\rangle_k \leftrightarrow |e\rangle_k$ $(k = a,b)$ is coupled to a pair of laser pulses possessing Rabi frequencies $\Omega_{kg(f)}(t)$ and $\Omega^{'}_{kg(f)}(t)$ with a red detuning Δ_k and a blue detuning $\Delta^{'}_k$, respectively. Besides, transition $|r\rangle_k \leftrightarrow |e\rangle_k$ is coupled to a pair of laser pulses possessing Rabi frequencies $\Omega_{kr}(t)$ and $\Omega^{'}_{kr}(t)$ with a blue detuning Δ_k and a red detuning $\Delta^{'}_k$, respectively. Here, we assume the Rabi frequencies $\Omega_{kg}(t)$, $\Omega_{kf}(t)$ and $\Omega_{kr}(t)$ are all real valued for simplicity. Two atoms interact with each other with Rydberg-mediated interaction with strength V when they are both in Rydberg states. In the interaction picture, the Hamiltonian of the system can be written as ($\hbar = 1$)

$$\begin{aligned} H_I(t) = \sum_{k=a,b} \{ & [\Omega_{kg}(t)e^{i\Delta_k t} + \Omega^{'}_{kg}(t)e^{-i\Delta^{'}_k t}]|g\rangle_k\langle e| \\ & + [\Omega_{kf}(t)e^{i\Delta_k t} + \Omega^{'}_{kf}(t)e^{-i\Delta^{'}_k t}]|f\rangle_k\langle e| \\ & + [\Omega_{kr}(t)e^{i\Delta_k t} + \Omega^{'}_{kr}(t)e^{-i\Delta^{'}_k t}]|r\rangle_k\langle e| + \text{H.c.}\} \\ & + V|rr\rangle_{ab}\langle rr|. \end{aligned} \tag{3}$$

Then, we assume $\Omega_{kg}(t) = \Omega_{k0}(t)\cos[\vartheta_k(t)]$, $\Omega^{'}_{kg}(t) = \Omega^{'}_{k0}(t)\cos[\vartheta_k(t)]$, $\Omega_{kf}(t) = \Omega_{k0}(t)\sin[\vartheta_k(t)]$, and $\Omega^{'}_{kf}(t) = \Omega^{'}_{k0}(t)\sin[\vartheta_k(t)]$. In the current scheme, ϑ_k is considered as a time-independent parameter. Thus, the Hamiltonian of the system can be written as

$$\begin{aligned} H_I(t) = \sum_{k=a,b} \{ & [\Omega_{k0}(t)e^{i\Delta_k t} + \Omega^{'}_{k0}(t)e^{-i\Delta^{'}_k t}]|+\rangle_k\langle e| \\ & + [\Omega_{kr}(t)e^{i\Delta_k t} + \Omega^{'}_{kr}(t)e^{-i\Delta^{'}_k t}]|r\rangle_k\langle e| + \text{H.c.}\} \\ & + V|rr\rangle_{ab}\langle rr|, \end{aligned} \tag{4}$$

where $|+\rangle_k = \cos\vartheta_k|g\rangle_k + \sin\vartheta_k|f\rangle$. Besides, we define $|-\rangle_k = \cos\vartheta_k|f\rangle_k - \sin\vartheta_k|g\rangle$, such that $\{|+\rangle_k,|-\rangle_k,|e\rangle_k, |r\rangle_k\}$ can form a complete orthogonal basis for atom k instead of $\{|g\rangle_k,|f\rangle_k,|e\rangle_k,|r\rangle_k\}$. In the current scheme, we set $\Delta_k = \Delta^{'}_k$ to help us cancel some Stark shifts when calculating the effective Hamiltonian. Considering conditions $\Omega_{k0}(t) = \Omega_{kr}(t) = \Omega^{'}_{k0}(t) = -\Omega^{'}_{kr}(t) = \Omega_k(t)$, and $|\Omega_k(t)| \ll \min\{\Delta_k,|\Delta_b - \Delta_a|,V\}$, if the system is initial in subspace $\mathcal{S}(0) = \{|{+}{+}\rangle_{ab},|{+}{-}\rangle_{ab},|{-}{+}\rangle_{ab},|{-}{-}\rangle_{ab}\}$, the effective Hamiltonian can be derived as

$$\begin{aligned} H_{\text{eff}}(t) = & \tilde{\Omega}_a(t)|r+\rangle_{ab}\langle{+}{+}| + \tilde{\Omega}_b(t)|+r\rangle_{ab}\langle{+}{+}| \\ & + \tilde{\Omega}_a(t)|{+}{-}\rangle_{ab}\langle r-| + \tilde{\Omega}_b(t)|{-}{+}\rangle_{ab}\langle -r| + \text{H.c.}, \end{aligned} \tag{5}$$

with effective Rabi frequency,

$$\tilde{\Omega}_k(t) = \frac{2\Omega_k^2(t)}{\Delta_k}. \tag{6}$$

The derivation of Eq. (5) is listed in the Appendix. In the following discussions, we assume the initial time is $t = 0$ and

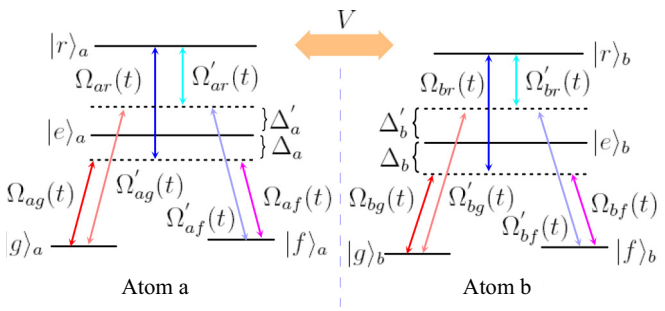

FIG. 1. Level configurations and pulse couplings of two atoms a and b with a Rydberg-Rydberg interaction V.

the final time is $t = T$. If we can achieve the gate operation,

$$U(\vartheta_a,\vartheta_b) = \begin{bmatrix} -1 & 0 & 0 & 0 \\ 0 & 1 & 0 & 0 \\ 0 & 0 & 1 & 0 \\ 0 & 0 & 0 & 1 \end{bmatrix}, \tag{7}$$

in the basis $\{|{+}{+}\rangle_{ab},|{+}{-}\rangle_{ab},|{-}{+}\rangle_{ab},|{-}{-}\rangle_{ab}\}$ at $t = T$, while ensuring that the condition for cyclic evolution (i) and the holonomic condition (ii) fulfilled, back to the basis $\{|gg\rangle_{ab},|gf\rangle_{ab},|fg\rangle_{ab},|ff\rangle_{ab}\}$, we can obtain

$$U(\vartheta_a,\vartheta_b) = \begin{bmatrix} \sin^2\vartheta_a - \cos^2\vartheta_a\cos 2\vartheta_b & -\cos^2\vartheta_a\sin 2\vartheta_b & -\sin 2\vartheta_a\cos^2\vartheta_b & -\frac{1}{2}\sin 2\vartheta_a\sin 2\vartheta_b \\ -\cos^2\vartheta_a\sin 2\vartheta_b & \cos^2\vartheta_a\cos 2\vartheta_b + \sin^2\vartheta_a & -\frac{1}{2}\sin 2\vartheta_a\sin 2\vartheta_b & -\sin 2\vartheta_a\sin^2\vartheta_b \\ -\sin 2\vartheta_a\cos^2\vartheta_b & -\frac{1}{2}\sin 2\vartheta_a\sin 2\vartheta_b & \cos^2\vartheta_a - \cos 2\vartheta_b\sin^2\vartheta_a & -\sin^2\vartheta_a\sin 2\vartheta_b \\ -\frac{1}{2}\sin 2\vartheta_a\sin 2\vartheta_b & -\sin 2\vartheta_a\sin^2\vartheta_b & -\sin^2\vartheta_a\sin 2\vartheta_b & \cos^2\vartheta_a + \sin^2\vartheta_a\cos 2\vartheta_b \end{bmatrix}. \tag{8}$$

For $\vartheta_a = \pi/2$, $\vartheta_b = \pi/2$, $U(\vartheta_a,\vartheta_b)$ becomes

$$U(\pi/2,\pi/2) = \begin{bmatrix} 1 & 0 & 0 & 0 \\ 0 & 1 & 0 & 0 \\ 0 & 0 & 1 & 0 \\ 0 & 0 & 0 & -1 \end{bmatrix}, \tag{9}$$

which is a holonomic controlled phase gate. While for $\vartheta_a = \pi/2$, $\vartheta_b = -\pi/4$, a holonomic controlled-NOT gate

$$U(\pi/2,-\pi/4) = \begin{bmatrix} 1 & 0 & 0 & 0 \\ 0 & 1 & 0 & 0 \\ 0 & 0 & 0 & 1 \\ 0 & 0 & 1 & 0 \end{bmatrix}, \tag{10}$$

can be realized. Therefore, for the sake of obtaining such a gate operation shown as Eq. (7), let us fully analyze dynamics governed by the effective Hamiltonian shown in Eq. (5). According to Eq. (5), the dynamics of system can be divided into four independent subspaces $\mathcal{S}_{e1} = \{|{+}{-}\rangle_{ab},|r{-}\rangle_{ab}\}$, $\mathcal{S}_{e2} = \{|{-}{+}\rangle_{ab},|{-}r\rangle_{ab}\}$, $\mathcal{S}_{e3} = \{|r{+}\rangle_{ab},|{+}{+}\rangle_{ab},|{+}r\rangle_{ab}\}$, and $\mathcal{S}_{e4} = \{|{-}{-}\rangle_{ab}\}$. Then, we have the following discussions.

(1) When the system is initial in state $|\phi_1(0)\rangle = |{+}{-}\rangle_{ab} \in \mathcal{S}_{e1}$, the evolution is governed by

$$H_{e1}(t) = \tilde{\Omega}_a(t)(|{+}{-}\rangle_{ab}\langle r{-}| + |r{-}\rangle_{ab}\langle{+}{-}|). \tag{11}$$

The evolution operator for $H_{e1}(t)$ can be directly given by

$$U_{e1}(t) = e^{-i\int_0^t H_{e1}(t')dt'}. \tag{12}$$

Thus the evolution of system is

$$|\phi_1(t)\rangle = U_{e1}(t)|{+}{-}\rangle_{ab} = \cos[\mu_1(t)]|{+}{-}\rangle_{ab} - i\sin[\mu_1(t)]|r{-}\rangle_{ab}, \tag{13}$$

where $\mu_1(t)$ reads

$$\mu_1(t) = \int_0^t \tilde{\Omega}_a(t')dt'. \tag{14}$$

Therefore, if $\mu_1(T) = 2k_1\pi$ $(k_1 = 0,1,2,\ldots)$ is satisfied, the evolution during time interval $[0,T]$ is $|\phi_1(0)\rangle = |{+}{-}\rangle_{ab} \to |\phi_1(T)\rangle = |{+}{-}\rangle_{ab}$.

(2) When the system is initial in state $|\phi_2(0)\rangle = |{-}{+}\rangle_{ab} \in \mathcal{S}_{e2}$, the evolution is governed by

$$H_{e2}(t) = \tilde{\Omega}_b(t)(|{-}{+}\rangle_{ab}\langle{-}r| + |{-}r\rangle_{ab}\langle{-}{+}|). \tag{15}$$

Similar to the discussions of subspace $\mathcal{S}_{e1}$ in case (1), the evolution of the system is

$$|\phi_2(t)\rangle = U_{e2}(t)|{-}{+}\rangle_{ab} = \cos[\mu_2(t)]|{-}{+}\rangle_{ab} - i\sin[\mu_2(t)]|r{-}\rangle_{ab}, \tag{16}$$

with

$$U_{e2}(t) = e^{-i\int_0^t H_{e2}(t')dt'}, \tag{17}$$

and

$$\mu_2(t) = \int_0^t \tilde{\Omega}_b(t')dt'. \tag{18}$$

By choosing $\mu_2(T) = 2k_2\pi$ $(k_2 = 0,1,2,\ldots)$, the evolution during the time interval $[0,T]$ is $|\phi_2(0)\rangle = |{-}{+}\rangle_{ab} \to |\phi_2(T)\rangle = |{-}{+}\rangle_{ab}$.

(3) When the system is initial in state $|\phi_3(0)\rangle = |{+}{+}\rangle_{ab} \in \mathcal{S}_{e3}$, the evolution is governed by

$$H_{e3}(t) = \tilde{\Omega}_a(t)|r{+}\rangle_{ab}\langle{+}{+}| + \tilde{\Omega}_b(t)|{+}r\rangle_{ab}\langle{+}{+}| + \text{H.c.} \tag{19}$$

In this case, the evolution of the system cannot be directly obtained. However, we can assume the evolution of the system described by an arbitrary three-dimensional vector,

$$|\phi_3(t)\rangle = U_{e3}(t)|{+}{+}\rangle_{ab} = e^{i\Theta_1}\sin\alpha\cos\beta|r{+}\rangle_{ab} + \cos\alpha|{+}{+}\rangle_{ab} + e^{i\Theta_2}\sin\alpha\sin\beta|{+}r\rangle_{ab}, \tag{20}$$

with α and β being two time-dependent parameters. Besides, take the holonomic condition (ii) shown in Eq. (2) into account, $\langle\phi_3(t)|H_{\text{eff}}(t)|\phi_3(t)\rangle$ should be satisfied for $t \in [0,T]$. This requires $\Theta_1,\Theta_2 = \pm\pi/2,\pm 3\pi/2,\pm 5\pi/2,\ldots$. Here, $\Theta_1 = \Theta_2 = -\pi/2$ is considered, such that

$$|\phi_3(t)\rangle = -i\sin\alpha\cos\beta|r{+}\rangle_{ab} + \cos\alpha|{+}{+}\rangle_{ab} - i\sin\alpha\sin\beta|{+}r\rangle_{ab}. \tag{21}$$

In Sec. II B, STA is introduced to achieve the pulse design for realizing the evolution $|\phi_3(0)\rangle = |{+}{+}\rangle_{ab} \rightarrow |\phi_3(T)\rangle = -|{+}{+}\rangle_{ab}$ in the time interval $[0,T]$. Meanwhile, the effective Rabi frequencies $\tilde{\Omega}_a(t)$ and $\tilde{\Omega}_b(t)$ designed by STA should make $\mu_1(T) = 2k_1\pi$ and $\mu_2(T) = 2k_2\pi$ both fulfilled.

(4) When the system is initial in state $|\phi_4(0)\rangle = |{-}{-}\rangle_{ab} \in \mathcal{S}_{e4}$, it is decoupled with the Hamiltonian shown in Eq. (5), thus the system remaining in state $|\phi_4(t)\rangle = |{-}{-}\rangle_{ab}$ during the time interval $[0,T]$.

According to the discussions above, we have

$$\begin{aligned}\sum_{l=1}^{4}|\phi_l(0)\rangle\langle\phi_l(0)| &= \sum_{l=1}^{4}|\phi_l(T)\rangle\langle\phi_l(T)| \\ &= |{+}{+}\rangle\langle{+}{+}| + |{+}{-}\rangle\langle{+}{-}| + |{-}{+}\rangle \\ &\quad \times \langle{-}{+}| + |{-}{-}\rangle\langle{-}{-}|, \end{aligned} \tag{22}$$

which makes the condition for cyclic evolution (i) fulfilled. On the other hand, it is easy to prove that $\langle\phi_l(t)|H_{\rm eff}(t)|\phi_{l'}(t)\rangle = 0$ $(l,l' = 1,2,3,4)$ is always satisfied, which means the holonomic condition (ii) is also fulfilled.

B. Designing pulses for the implementations of two-qubit logic gates via STA

In this part, we design pulses for the implementations of two-qubit logic gates via the STA method [95]. First, we briefly introduce the method [95]. Suppose that we intend to drive an N-dimensional system from its initial state $|\Psi_0\rangle$ to a target state $|\Psi_T\rangle$ along a moving state $|\xi_1(t)\rangle$ (i.e., $|\xi_1(0)\rangle = |\Psi_0\rangle, |\xi_1(T)\rangle = |\Psi_T\rangle$). To further construct a unitary evolution operator for the N-dimensional system, we introduce another $N-1$ state $|\xi_2(t)\rangle, |\xi_3(t)\rangle, \ldots, |\xi_N(t)\rangle$, such that $\{|\xi_p(t)\rangle | p = 1,2,\ldots,N\}$ forming a complete orthogonal basis (i.e., $\sum_p |\xi_p(t)\rangle\langle\xi_p(t)| = I_N$, where I_N denotes the identity operator for the N-dimensional system). Then, we can construct an evolution operator for the N-dimensional system as

$$U_N(t) = |\xi_1(t)\rangle\langle\xi_1(0)| + \sum_{p,q\neq 1}\lambda_{pq}(t)|\xi_p(t)\rangle\langle\xi_q(0)|, \tag{23}$$

where parameters $\{\lambda_{pq}(t)\}$ should satisfy

$$\sum_{s\neq 1}\lambda_{ps}(t)\lambda^*_{qs}(t) = \delta_{pq}\ (p,q \neq 1), \tag{24}$$

to ensure the unitary of $U_N(t)$ (i.e., $U_N(t)U_N^\dagger(t) = U_N^\dagger(t)U_N(t) = I_N$). It is easy to find that the evolution operator $U_N(t)$ makes sure the system evolves along $|\xi_1(t)\rangle$ when $|\xi_1(0)\rangle = |\Psi_0\rangle$. On the other hand, consider the Schrödinger equation,

$$i\dot{U}_N(t) = H_N(t)U_N(t), \tag{25}$$

one can derive the Hamiltonian $H_N(t)$ of the N-dimensional system as

$$\begin{aligned} H_N(t) &= i\dot{U}_N(t)U_N^\dagger(t) \\ &= i\sum_{d=1}^{N}|\dot{\xi}_d(t)\rangle\langle\xi_d(t)| \\ &\quad + i\sum_{p,q,s\neq 1}\dot{\lambda}_{ps}(t)\lambda^*_{qs}(t)|\xi_p(t)\rangle\langle\xi_q(t)|, \end{aligned} \tag{26}$$

where the condition shown in Eq. (24) is used in the derivation.

Now applying the above method to the current scheme and considering the subspace $\{|r{+}\rangle_{ab}, |{+}{+}\rangle_{ab}, |{+}r\rangle_{ab}\}$ $(N = 3)$ of case (3) of Sec. II A, we select

$$\begin{aligned} |\xi_1(t)\rangle &= -i\sin\alpha\cos\beta|r{+}\rangle_{ab} + \cos\alpha|{+}{+}\rangle_{ab} \\ &\quad - i\sin\alpha\sin\beta|{+}r\rangle_{ab}, \\ |\xi_2(t)\rangle &= i\cos\alpha\cos\beta|r{+}\rangle_{ab} + \sin\alpha|{+}{+}\rangle_{ab} \\ &\quad + i\cos\alpha\sin\beta|{+}r\rangle_{ab}, \\ |\xi_3(t)\rangle &= i\sin\beta|r{+}\rangle_{ab} - i\cos\beta|{+}r\rangle_{ab}, \end{aligned} \tag{27}$$

and

$$\begin{aligned} \lambda_{22}(t) &= \cos\theta, \quad \lambda_{23}(t) = -\sin\theta, \\ \lambda_{32}(t) &= \sin\theta, \quad \lambda_{33}(t) = \cos\theta, \end{aligned} \tag{28}$$

where $|\xi_1(t)\rangle = |\phi_3(t)\rangle$ and θ is a time-dependent parameter. Substituting Eqs. (27) and (28) into Eq. (26), we obtain

$$\begin{aligned} H_3(t) &= (\dot{\alpha}\cos\beta - \dot{\theta}\sin\alpha\sin\beta)(|{+}{+}\rangle_{ab}\langle r{+}| + |r{+}\rangle_{ab} \\ &\quad \times \langle{+}{+}|) + (\dot{\alpha}\sin\beta + \dot{\theta}\sin\alpha\cos\beta)(|{+}{+}\rangle_{ab} \\ &\quad \langle{+}r| + |{+}r\rangle_{ab} \times \langle{+}{+}|) + i(\dot{\beta} - \dot{\theta}\cos\alpha)(|{+}r\rangle_{ab} \\ &\quad \times \langle r{+}| - |r{+}\rangle_{ab}\langle{+}r|). \end{aligned} \tag{29}$$

Comparing $H_3(t)$ in Eq. (29) with $H_{e3}(t)$ in Eq. (19), we set

$$\begin{aligned} \tilde{\Omega}_a(t) &= \dot{\alpha}\cos\beta - \dot{\theta}\sin\alpha\sin\beta, \\ \tilde{\Omega}_b(t) &= \dot{\alpha}\sin\beta + \dot{\theta}\sin\alpha\cos\beta, \\ \dot{\beta} &= \dot{\theta}\cos\alpha \end{aligned} \tag{30}$$

to make $H_3(t) = H_{e3}(t)$ satisfied. When the system is initial in $|{+}{+}\rangle_{ab}$, by selecting $\alpha(0) = 0$, $\alpha(T) = (2k_3+1)\pi$ $(k_3 = 0,1,2,3,\ldots)$, the system would evolve from $|{+}{+}\rangle$ to $-|{+}{+}\rangle$ along state $|\xi_1(t)\rangle$ $(|\phi_3(t)\rangle)$ in time interval $[0,T]$. Besides, we add condition $\dot{\alpha}(0) = \dot{\alpha}(T) = \dot{\theta}(0) = \dot{\theta}(T) = 0$, such that $\tilde{\Omega}_a(0) = \tilde{\Omega}_a(T) = \tilde{\Omega}_b(0) = \tilde{\Omega}_b(T) = 0$ is fulfilled. Therefore, parameters α and $\dot{\theta}$ can be chosen as

$$\begin{aligned} \alpha &= \frac{(2k_3+1)\pi}{2}\left[1 - \cos\left(\frac{\pi t}{T}\right)\right], \\ \dot{\theta} &= \frac{\Upsilon_1 t}{T^2} + \frac{\Upsilon_2 t^2}{T^3} - \frac{(\Upsilon_1+\Upsilon_2)t^3}{T^4}, \end{aligned} \tag{31}$$

where Υ_1 and Υ_2 are two time-independent parameters. With Eq. (31), parameter β can be solved by calculating

$$\beta(t) = \beta(0) + \int_0^t \dot{\theta}(t')\cos[\alpha(t')]dt'. \tag{32}$$

Until now, effective Rabi frequencies $\tilde{\Omega}_a(t)$ and $\tilde{\Omega}_b(t)$ with the parameters given in Eqs. (31) and (32) can make the system evolve along $|\xi_1(t)\rangle$ from $|{+}{+}\rangle$ to $-|{+}{+}\rangle$ with arbitrary Υ_1 and Υ_2. Next, we should select suitable values of Υ_1 and Υ_2 to make conditions $\mu_1(T) = 2k_1\pi$ and $\mu_2(T) = 2k_2\pi$ fulfilled. Here, the numerical integrations are adopted to find suitable

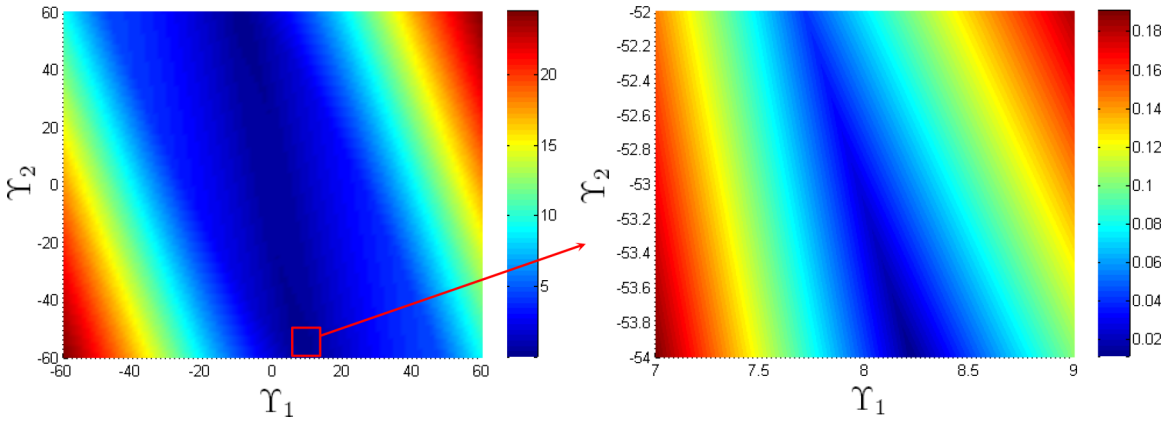

FIG. 2. $G(\Upsilon_1,\Upsilon_2)$ versus Υ_1 and Υ_2.

Υ_1 and Υ_2. Defining a function,

$$G(\Upsilon_1,\Upsilon_2) = |\mu_1(T) - 2k_1\pi| + |\mu_2(T) - 2k_2\pi|, \quad (33)$$

if $G(\Upsilon_1,\Upsilon_2) = 0$, conditions $\mu_1(T) = 2k_1\pi$ and $\mu_2(T) = 2k_2\pi$ are accurately fulfilled. However, if it is difficult to find Υ_1 and Υ_2 to make $G(\Upsilon_1,\Upsilon_2) = 0$ in a range, one may try to select Υ_1 and Υ_2 to make $G(\Upsilon_1,\Upsilon_2)$ as tiny as possible. When considering $k_1 = k_2 = k_3 = 1$ and $\beta(0) = \pi/4$, $G(\Upsilon_1,\Upsilon_2)$ versus Υ_1 and Υ_2 is plotted in Fig. 2. According to Fig. 2, we choose $\Upsilon_1 = 8.222$ and $\Upsilon_2 = -53.996$, where we can get $G(\Upsilon_1,\Upsilon_2) = 0.0115$, a value very close to zero. With chosen Υ_1 and Υ_2, the effective Rabi frequencies $\tilde{\Omega}_a(t)$ and $\tilde{\Omega}_b(t)$ versus t/T are plotted in Fig. 3. According to Fig. 3, we obtain the maximal value of the effective Rabi frequencies as $\tilde{\Omega}_{\text{effm}} = \max_{0\leqslant t\leqslant T}\{\tilde{\Omega}_a(t),\tilde{\Omega}_b(t)\} = 15/T$.

To check that the effective Hamiltonian can realize an operation of the two-qubit logic gate shown in Eq. (7), we define the fidelity for the effective dynamics as

$$F_e(\varphi_a,\varphi_b) = |\langle\Psi_T(\varphi_a,\varphi_b)|U_e(T)|\Psi_0(\varphi_a,\varphi_b)\rangle|^2, \quad (34)$$

where $U_e(T)$ is the evolution operator of the effective dynamics with designed effective Rabi frequencies $\tilde{\Omega}_a(t)$ and $\tilde{\Omega}_b(t)$ for the time interval $[0,T]$,

$$\begin{aligned}|\Psi_0(\varphi_a,\varphi_b)\rangle &= \cos\varphi_a\cos\varphi_b|{+}{+}\rangle_{ab} + \cos\varphi_a\sin\varphi_b|{+}{-}\rangle_{ab} \\ &+ \sin\varphi_a\cos\varphi_b|{-}{+}\rangle_{ab} + \sin\varphi_a\sin\varphi_b|{-}{-}\rangle_{ab}, \quad (35)\end{aligned}$$

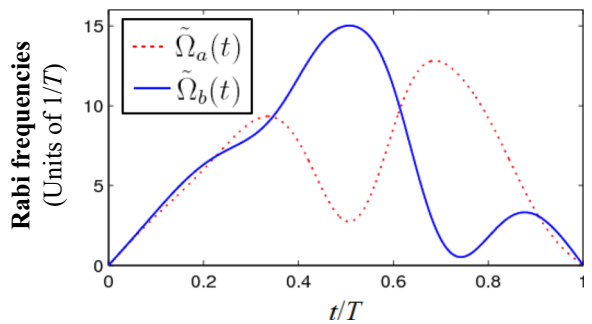

FIG. 3. The effective Rabi frequencies $\tilde{\Omega}_a(t)$ and $\tilde{\Omega}_b(t)$ versus t/T.

is the initial state of the system, and

$$\begin{aligned}|\Psi_T(\varphi_a,\varphi_b)\rangle &= -\cos\varphi_a\cos\varphi_b|{+}{+}\rangle_{ab} + \cos\varphi_a\sin\varphi_b|{+}{-}\rangle_{ab} \\ &+ \sin\varphi_a\cos\varphi_b|{-}{+}\rangle_{ab} + \sin\varphi_a\sin\varphi_b|{-}{-}\rangle_{ab}, \quad (36)\end{aligned}$$

denotes the final state after an ideal gate operation. $1 - F_e(\varphi_a,\varphi_b)$ versus $\varphi_a/2\pi$ and $\varphi_b/2\pi$ is plotted in Fig. 4. As shown in Fig. 4, $1 - F_e(\varphi_a,\varphi_b)$ takes tiny values for different φ_a and φ_b. Besides, seen from Fig. 4, we have $\max_{\varphi_a,\varphi_b}[1 - F_e(\varphi_a,\varphi_b)] = 1.4175 \times 10^{-4}$. Moreover, we consider the average effective fidelity [120],

$$\bar{F}_e = \frac{1}{4\pi^2}\int_0^{2\pi}\int_0^{2\pi} F_e(\varphi_a,\varphi_b)d\varphi_a d\varphi_b. \quad (37)$$

Numerical integration of Eq. (37) indicates that $1 - \bar{F}_e = 3.58 \times 10^{-5}$.

III. NUMERICAL SIMULATIONS

In this section, we investigate the feasibility of the scheme via numerical simulations. Here, the controlled phase gate ($\vartheta_a = \pi/2$, $\vartheta_b = \pi/2$) is taken as an example in the following discussions. Before we begin the discussions, we define the

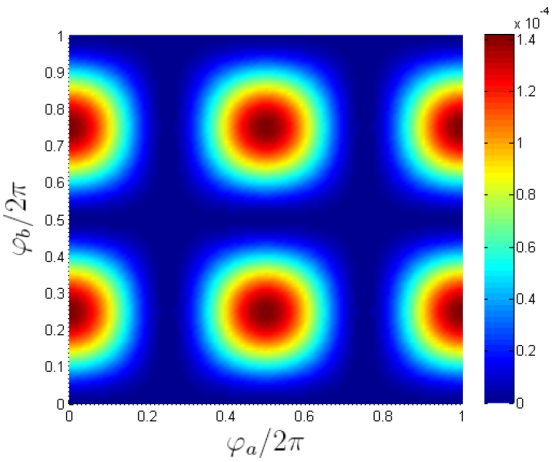

FIG. 4. $1 - F_e(\varphi_a,\varphi_b)$ versus $\varphi_a/2\pi$ and $\varphi_b/2\pi$.

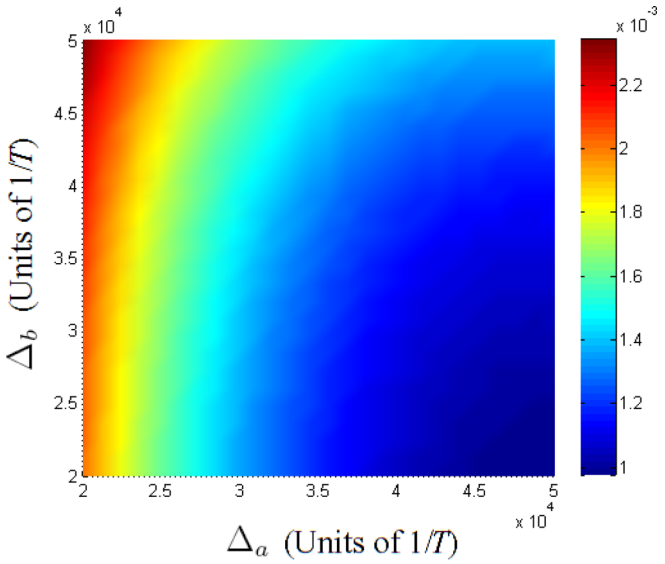

FIG. 5. $1-\bar{F}_{\rm cp}$ versus Δ_a and Δ_b ($V=\sqrt{2\Delta_a\tilde{\Omega}_{\rm effm}}$).

fidelity of the controlled phase gate as

$$F_{\rm cp}(\eta_a,\eta_b)=|\langle\Phi_{{\rm cp}T}(\eta_a,\eta_b)|U_{\rm cp}(T)|\Phi_0(\eta_a,\eta_b)\rangle|^2, \quad (38)$$

where $U_{\rm cp}(T)$ and $F_{\rm cp}(\eta_a,\eta_b)$ are the evolution operator for the time interval $[0,T]$ and the fidelity with corresponding gate operation, respectively. Moreover, the initial state can be described by

$$\begin{aligned}|\Phi_0(\eta_a,\eta_b)\rangle &= \cos\eta_a\cos\eta_b|gg\rangle_{ab}+\cos\eta_a\sin\eta_b|gf\rangle_{ab}\\ &+\sin\eta_a\cos\eta_b|fg\rangle_{ab}+\sin\eta_a\sin\eta_b|ff\rangle_{ab}.\end{aligned} \quad (39)$$

On the other hand, the final state after ideal gate operations of the controlled phase gate can be written as

$$\begin{aligned}|\Phi_{{\rm cp}T}(\eta_a,\eta_b)\rangle &= \cos\eta_a\cos\eta_b|gg\rangle_{ab}+\cos\eta_a\sin\eta_b|gf\rangle_{ab}\\ &+\sin\eta_a\cos\eta_b|fg\rangle_{ab}-\sin\eta_a\sin\eta_b|ff\rangle_{ab}.\end{aligned} \quad (40)$$

As an index to check the performance of the scheme with a different initial state, the average fidelity [120],

$$\bar{F}_{\rm cp}=\frac{1}{4\pi^2}\int_0^{2\pi}\int_0^{2\pi}F_{\rm cp}(\eta_a,\eta_b)d\eta_a d\eta_b, \quad (41)$$

would be mainly considered in the following discussions.

To derive Rabi frequencies $\Omega_{kg}(t)$, $\Omega_{kf}(t)$, and $\Omega_{kr}(t)$ from effective Rabi frequencies $\tilde{\Omega}_a(t)$ and $\tilde{\Omega}_b(t)$, we should first make a choice of detunings Δ_a and Δ_b. Therefore, we plot $1-\bar{F}_{\rm cp}$ versus Δ_a and Δ_b in Fig. 5. Here, we consider $V=\sqrt{2\Delta_a\tilde{\Omega}_{\rm effm}}$ for the Rydberg blockade in the numerical simulation, which is fourfold to the maximal value of Rabi frequencies $\Omega_a(t)$ and $\Omega_b(t)$. Seen from Fig. 5, the average fidelity $\bar{F}_{\rm cp}$ gets close to 1 gradually when detunings Δ_a and Δ_b increase. Because when detunings are becoming larger, the dynamics of the system is even approaching the effective

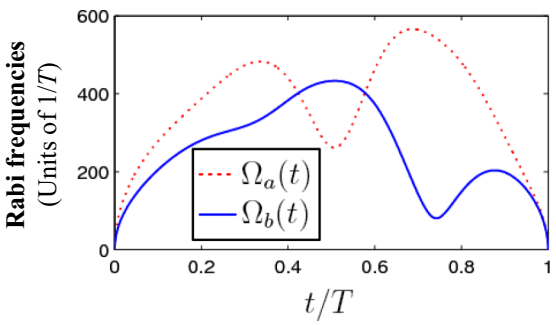

FIG. 6. $\Omega_a(t)$ and $\Omega_b(t)$ versus t/T.

dynamics governed by the effective Hamiltonian shown in Eq. (5), and thus the average fidelity $\bar{F}_{\rm cp}$ is getting close to the effective average fidelity $\bar{F}_e$ simultaneously. Here, we consider $\Delta_a=5\times10^4/T$ and $\Delta_b=2.5\times10^4/T$, and plot $\Omega_a(t)$ and $\Omega_b(t)$ versus t/T in Fig. 6. The maximal value of Rabi frequencies $\Omega_a(t)$ and $\Omega_b(t)$ reading from Fig. 6 is $\Omega_{\rm max}=\max_{0\leqslant t\leqslant T}\{\Omega_a(t),\Omega_b(t)\}=566/T$. In this case, the average fidelity is $\bar{F}_{\rm cp}=0.9990$. Additionally, we consider the influence to the average fidelity due to the fluctuation δV of Rydberg-mediated interaction strength V. $1-\bar{F}_{\rm cp}$ versus $\delta V/V$ with $\Delta_a=5\times10^4/T$ and $\Delta_b=2.5\times10^4/T$ is plotted in Fig. 7. As shown in Fig. 7, when $|\delta V/V|\leqslant 20\%$, the change of the average fidelity $\bar{F}_{\rm cp}$ is less than 4×10^{-4}, which indicates the performance of the controlled phase gate suffers little from the fluctuation of the Rydberg-mediated interaction strength V. Moreover, the average fidelity $\bar{F}_{\rm cp}$, tends to increase when the Rydberg-mediated interaction with strength V increases. Thus, increasing V may be a choice to improve the performance of the controlled phase gate.

In real experiments, there may exist several kinds of noise, which disturb wave shapes of Rabi frequencies of pulses. It is worthwhile to study the influences caused by the noise. Here, we investigate two typical kinds of noise, the random noise of pulse amplitudes and the additive white Gaussian noise (AWGN). For the controlled phase gate ($\vartheta_a=\pi/2,\vartheta_b=\pi/2$), we have $\Omega_{kg}=\Omega'_{kg}=0$ ($k=a,b$). Therefore, only noise acting on $\Omega_{k_J}(t)$ ($J=f,r$) is considered.

Random noise of pulse amplitudes. The Rabi frequencies under the influence of the random noise of pulse amplitudes

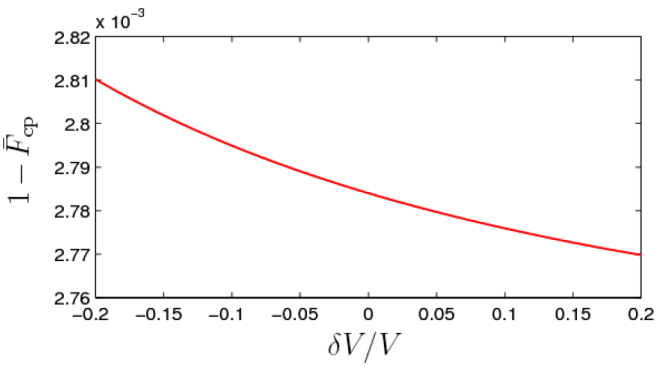

FIG. 7. $1-\bar{F}_{\rm cp}$ versus $\delta V/V$ ($\Delta_a=5\times10^4/T$ and $\Delta_b=2.5\times10^4/T$).

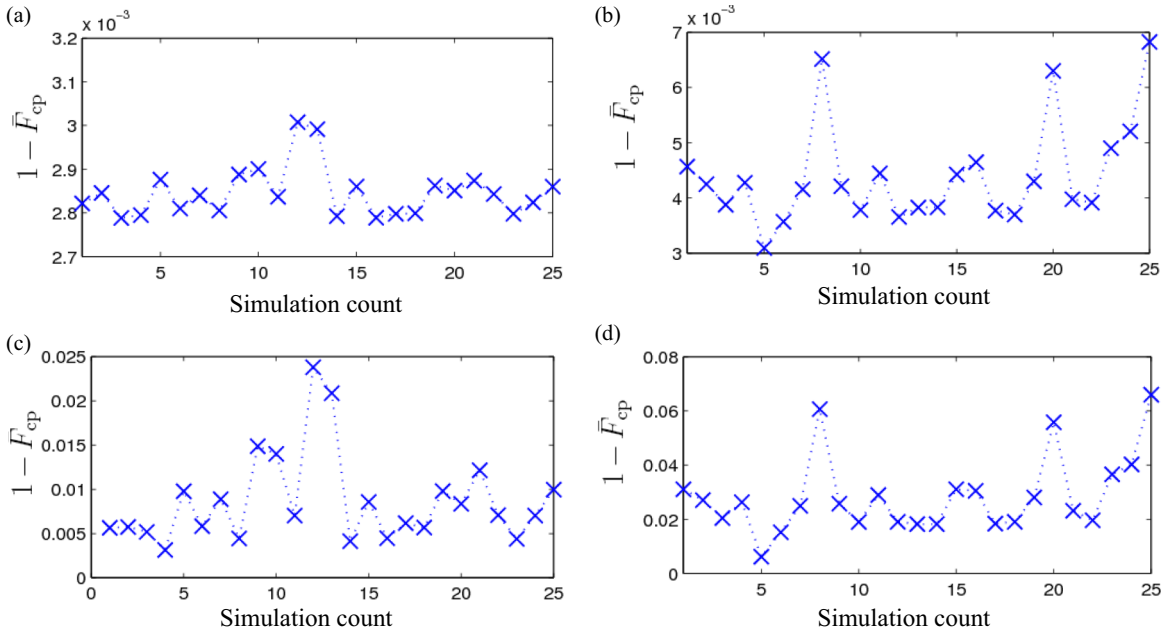

FIG. 8. $1-\bar{F}_{\rm cp}$ versus simulation count with (a) $\Lambda_{kJ}=\Lambda_{kJ}^{'}=0.01$, (b) $\Lambda_{kJ}=\Lambda_{kJ}^{'}=0.05$, (c) $\Lambda_{kJ}=\Lambda_{kJ}^{'}=0.1$, and (d) $\Lambda_{kJ}=\Lambda_{kJ}^{'}=0.2$.

can be described as

$$\breve{\Omega}_{kJ}(t)=[1+\mathrm{rand}_{kJ}(t,\Lambda_{kJ})]\Omega_{kJ}(t),$$
$$\breve{\Omega}_{kJ}^{'}(t)=[1+\mathrm{rand}_{kJ}^{'}(t,\Lambda_{kJ}^{'})]\Omega_{kJ}(t), \tag{42}$$

where $\mathrm{rand}_{kJ}(t,\Lambda_{kJ})$ ($\mathrm{rand}_{kJ}^{'}(t,\Lambda_{kJ}^{'})$) denotes a random function with the amplitude Λ_{kJ} ($\Lambda_{kJ}^{'}$), i.e., $\mathrm{rand}_{kJ}(t,\Lambda_{kJ})$ ($\mathrm{rand}_{kJ}^{'}(t,\Lambda_{kJ}^{'})$) generates a random number in the interval $[-\Lambda_{kJ},\Lambda_{kJ}]$ ($[-\Lambda_{kJ}^{'},\Lambda_{kJ}^{'}]$) at time t. Since the noise is random in the simulations, one is required to perform simulations several times for estimating the influences of the noise. Here, we perform numerical simulations based on the Rabi frequencies shown in Eq. (42) 25 times (for each group of noise amplitudes), and plot the $1-\bar{F}_{\rm cp}$ versus simulation count in Figs. 8(a) and 8(d) with (a) $\Lambda_{kJ}=\Lambda_{kJ}^{'}=0.01$, (b) $\Lambda_{kJ}=\Lambda_{kJ}^{'}=0.05$, (c) $\Lambda_{kJ}=\Lambda_{kJ}^{'}=0.1$, and (d) $\Lambda_{kJ}=\Lambda_{kJ}^{'}=0.2$, respectively. According to Figs. 8(a)–8(c), one can obtain $1-\bar{F}_{\rm cp}\sim 10^{-3}$ when $\Lambda_{kJ},\Lambda_{kJ}^{'}\leqslant 0.1$. Even when Λ_{kJ} and $\Lambda_{kJ}^{'}$ reach 0.2, the average fidelity $\bar{F}_{\rm cp}$ may still be higher than 0.9. Generally speaking, the scales of noise are usually much weaker compared with the amplitudes of original pulses. Thus, the controlled phase gate could be quite robust against the noise of pulse amplitudes.

Additive white Gaussian noise (AWGN). The Rabi frequencies under the influence of the AWGN of pulse amplitudes can be described as

$$\Omega_{kJ}^{\triangle}(t)=\Omega_{kJ}(t)+\mathrm{awgn}(\Omega_{kJ}(t),R_{SNkJ}),$$
$$\Omega_{kJ}^{'\triangle}(t)=\Omega_{kJ}^{'}(t)+\mathrm{awgn}(\Omega_{kJ}^{'}(t),R_{SNkJ}^{'}), \tag{43}$$

where $\mathrm{awgn}(\Omega_{kJ}(t),R_{SNkJ})$ ($\mathrm{awgn}(\Omega_{kJ}^{'}(t),R_{SBkJ})$) is the function generating AWGN with signal-to-noise ratio R_{SNkJ} ($R_{SNkJ}^{'}$) for pulses $\Omega_{kJ}(t)$ ($\Omega_{kJ}^{'}(t)$). The signal-to-noise ratios indicate the ratio between the original Rabi frequencies and the scales of noise. Based on Eq. (43), signal-to-noise ratios (a) $R_{SNkJ}=R_{SNkJ}^{'}=10$, (b) $R_{SNkJ}=R_{SNkJ}^{'}=5$, (c) $R_{SNkJ}=R_{SNkJ}^{'}=2$, and (d) $R_{SNkJ}=R_{SNkJ}^{'}=1$ are considered. For each group of signal-to-noise ratios, 25 numerical simulations for $1-\bar{F}_{\rm cp}$ are performed, and the results for corresponding signal-to-noise ratios are plotted in Figs. 9(a)–9(d), respectively. According to Figs. 9(a)–9(c), $1-\bar{F}_{\rm cp}\sim 10^{-3}$ can be obtained when $R_{SNkJ},R_{SNkJ}^{'}=2$. Moreover, as shown in Fig. 9(d), in the case of $R_{SNkJ}=R_{SNkJ}^{'}=1$, where the scales of noise are similar to the original Rabi frequencies, $1-\bar{F}_{\rm cp}$ can still reach $10^{-3}\sim 10^{-2}$. Comparing the results of AWGN with the results of the noise of pulse amplitudes, the scheme is more robust against AWGN than the noise of pulse amplitudes.

Another disturbing factor in real experiments is the decoherence. In the current scheme, the main decoherence factors are the atomic spontaneous emission from the Rydberg state $|r\rangle_k$ to the intermediate state $|e\rangle_k$ with spontaneous emission rate γ_{kr} and that from the intermediate state $|e\rangle_k$ to the ground state $|g\rangle_k$ ($|f\rangle_k$) with spontaneous emission rate γ_{kg} (γ_{kf}). As shown by many previous schemes [120–122] that the Lindblad master equation with the Markov approximation is an effective model to describe the quantum evolution when the atom-cavity coupled system is interacted with a thermal reservoir, as the reservoir is typically an extended open system with many degrees of freedom. For the current scheme, considering the decoherence factors discussed above, the evolution should be described by a master equation as

$$\dot{\rho}(t)=i[\rho(t),H(t)]+\sum_{\iota=1}^{6}\Big[L_\iota\rho L_\iota^\dagger-\frac{1}{2}(L_\iota^\dagger L_\iota\rho+\rho L_\iota^\dagger L_\iota)\Big], \tag{44}$$

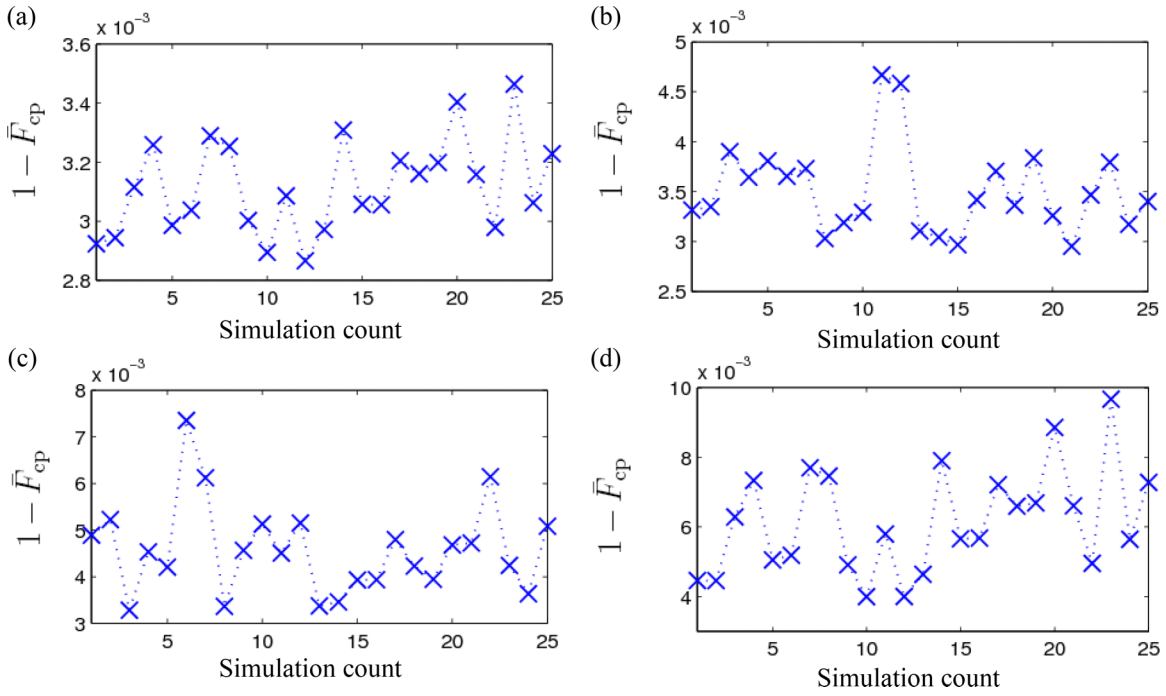

FIG. 9. $1-\bar{F}_{cp}$ versus simulation count with signal-to-noise ratios (a) $R_{SNk_J}=R'_{SNk_J}=10$, (b) $R_{SNk_J}=R'_{SNk_J}=5$, (c) $R_{SNk_J}=R'_{SNk_J}=2$, and (d) $R_{SNk_J}=R'_{SNk_J}=1$.

where, Lindblad operators $\{L_\iota|\iota=1,2,3,\ldots,6\}$ read

$$L_1=\sqrt{\gamma_{ar}}|e\rangle_a\langle r|,\ L_2=\sqrt{\gamma_{br}}|e\rangle_b\langle r|,$$
$$L_3=\sqrt{\gamma_{ag}/2}|e\rangle_a\langle g|,\ L_4=\sqrt{\gamma_{bg}/2}|e\rangle_b\langle g|,$$
$$L_5=\sqrt{\gamma_{af}/2}|e\rangle_a\langle r|,\ L_6=\sqrt{\gamma_{bf}/2}|e\rangle_b\langle r|. \quad (45)$$

When the decoherence is considered, the fidelity of the controlled phase gate with initial state $|\Phi_0(\eta_a,\eta_b)\rangle$ can be derived using

$$F_{cp}(\eta_a,\eta_b)=|\langle\Phi_{cpT}(\eta_a,\eta_b)|\rho(\eta_a,\eta_b,T)|\Phi_{cpT}(\eta_a,\eta_b)\rangle|^2, \quad (46)$$

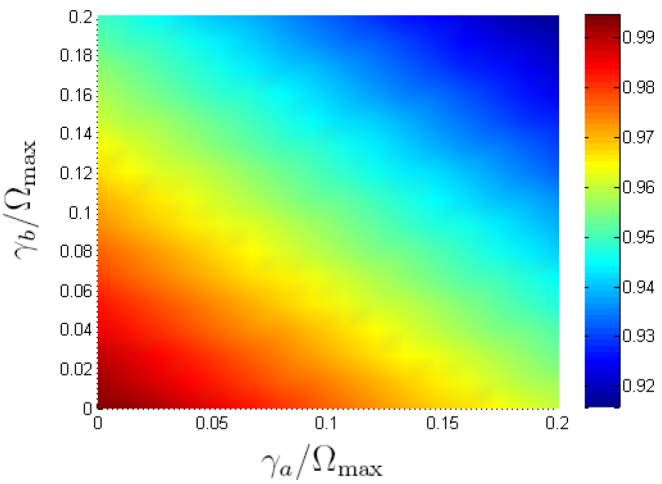

FIG. 10. $1-\bar{F}_{cp}$ versus γ_a/Ω_{max} and γ_b/Ω_{max}.

with $\rho(\eta_a,\eta_b,T)$ being the density operator of the system at time T with initial state $|\Phi_0(\eta_a,\eta_b)\rangle$. The average fidelity $\bar{F}_{cp}$ can still be calculated by using Eq. (41). Generally, the Rydberg state $|r\rangle$ is more stable than the intermediate state $|e\rangle$. The spontaneous emission rates $\gamma_{kr}\sim$ kHz and $\gamma_{kg},\gamma_{kf}\sim$ MHz have been shown in schemes [118,120–122]. Therefore, we assume $\gamma_{kg}=\gamma_{kf}=\gamma_{kr}\times10^3=\gamma_k$ in the following. $1-\bar{F}_{cp}$ versus γ_a/Ω_{max} and γ_b/Ω_{max} is plotted in Fig. 10. Seen from Fig. 10, the average fidelity $\bar{F}_{cp}$ falls when γ_a and γ_b increase, while for $\gamma_a/\Omega_{max},\gamma_b/\Omega_{max}\leqslant0.5$, the average fidelity $\bar{F}_{cp}$ keeps higher than 0.9140. Moreover, considering a group of parameters $V=20$ MHz, $\Delta_a=441.7$ MHz, $\Delta_b=220.8$ MHz, $\Omega_{max}=5$ MHz, $\gamma_a=\gamma_b=1$ MHz ($\gamma_a/\Omega_{max}=\gamma_b/\Omega_{max}=0.2$) [118,120], we obtain $\bar{F}_{cp}=0.9158$. To obtain a relative high average fidelity, one may try to intensify the maximal value of Rabi frequencies. Besides, one may also adjust the detunings of couplings to restrain the populations of the intermediate states for higher fidelities of gates.

IV. DISCUSSIONS AND CONCLUSION

In conclusion, we have proposed a scheme for realizing nonadiabatic holonomic computation assisted by two atoms and STA. The physical model can be built by ^{87}Rb atoms with $|g\rangle=|5s_{1/2},F=1,M_F=1\rangle$, $|f\rangle=|5s_{1/2},F=2,M_F=2\rangle$, $|e\rangle=|5p_{1/2},F=2,M_F=2\rangle$, and $|r\rangle=|58d_{3/2},F=3,M_F=3\rangle$ [118,123]. The blockade effect induced by strong Rydberg-mediated interaction between two Rydberg atoms allows us to simplify the dynamics of the system and obtain an effective Hamiltonian. Based on the effective Hamiltonian, the STA is applied in designing pulses, which produces high fidelity of holonomic quantum

gates without using adiabatic passages. Numerical simulations showed that the scheme is robust against the random noise of pulse amplitudes, the AWGN, and the atomic spontaneous emissions. Thus, the scheme may provide an alternative approach toward robust nonadiabatic holonomic computation.

ACKNOWLEDGMENTS

This work was supported by the National Natural Science Foundation of China under Grants No. 11575045, No. 11374054, No. 11674060, and No. 11747011.

APPENDIX: DERIVATION OF THE EFFECTIVE HAMILTONIAN OF EQ. (5)

According to the Hamiltonian shown in Eq. (4), the system evolves in Hilbert space spanned by

$$|\psi_1\rangle = |{+}{+}\rangle_{ab},\quad |\psi_2\rangle = |{+}{-}\rangle_{ab},\quad |\psi_3\rangle = |{+}e\rangle_{ab},\quad |\psi_4\rangle = |{+}r\rangle_{ab},\quad |\psi_5\rangle = |{-}{+}\rangle_{ab},\quad |\psi_6\rangle = |{-}{-}\rangle_{ab},$$
$$|\psi_7\rangle = |{-}e\rangle_{ab},\quad |\psi_8\rangle = |{-}r\rangle_{ab},\quad |\psi_9\rangle = |e{+}\rangle_{ab},\quad |\psi_{10}\rangle = |e{-}\rangle_{ab},\quad |\psi_{11}\rangle = |ee\rangle_{ab},\quad |\psi_{12}\rangle = |er\rangle_{ab},\quad |\psi_{13}\rangle = |r{+}\rangle_{ab},$$
$$|\psi_{14}\rangle = |r{-}\rangle_{ab},\quad |\psi_{15}\rangle = |re\rangle_{ab},\quad |\psi_{16}\rangle = |rr\rangle_{ab}. \tag{A1}$$

Thus, the Hamiltonian shown in Eq. (4) can be rewritten as

$$\begin{aligned} H(t) = {} & [\Omega_{a0}(t)e^{i\Delta_a t} + \Omega_{a0}^{'}(t)e^{-i\Delta_a t}](|\psi_1\rangle\langle\psi_9| + |\psi_2\rangle\langle\psi_{10}| + |\psi_3\rangle\langle\psi_{11}| + |\psi_4\rangle\langle\psi_{12}|) \\ & + [\Omega_{ar}(t)e^{i\Delta_a t} + \Omega_{ar}^{'}(t)e^{-i\Delta_a t}](|\psi_{13}\rangle\langle\psi_9| + |\psi_{14}\rangle\langle\psi_{10}| + |\psi_{15}\rangle\langle\psi_{11}| + |\psi_{16}\rangle\langle\psi_{12}|) \\ & + [\Omega_{b0}(t)e^{i\Delta_b t} + \Omega_{b0}^{'}(t)e^{-i\Delta_b t}](|\psi_1\rangle\langle\psi_3| + |\psi_5\rangle\langle\psi_7| + |\psi_9\rangle\langle\psi_{11}| + |\psi_{13}\rangle\langle\psi_{15}|) \\ & + [\Omega_{br}(t)e^{i\Delta_b t} + \Omega_{br}^{'}(t)e^{-i\Delta_b t}](|\psi_4\rangle\langle\psi_3| + |\psi_8\rangle\langle\psi_7| + |\psi_{12}\rangle\langle\psi_{11}| + |\psi_{16}\rangle\langle\psi_{15}|) \\ & + \text{H.c.} + V|\psi_{16}\rangle\langle\psi_{16}|. \end{aligned} \tag{A2}$$

By introducing a picture transformation with unitary operator $R(t) = e^{-iVt|\psi_{16}\rangle\langle\psi_{16}|}$, one can move to another picture where the Hamiltonian is

$$H'(t) = R^{\dagger}(t)H(t)R(t) - iR^{\dagger}(t)\dot{R}(t) = \sum_{n=1}^{4} h_n^{\dagger}(t)e^{i\omega_n t} + h_n(t)e^{-i\omega_n t}, \tag{A3}$$

with

$$\begin{aligned} h_1(t) = {} & \Omega_{a0}(t)(|\psi_9\rangle\langle\psi_1| + |\psi_{10}\rangle\langle\psi_2| + |\psi_{11}\rangle\langle\psi_3| + |\psi_{12}\rangle\langle\psi_4|) + \Omega_{a0}^{'}(t)(|\psi_1\rangle\langle\psi_9| + |\psi_2\rangle\langle\psi_{10}| + |\psi_3\rangle\langle\psi_{11}| + |\psi_4\rangle\langle\psi_{12}|) \\ & + \Omega_{ar}(t)(|\psi_9\rangle\langle\psi_{13}| + |\psi_{10}\rangle\langle\psi_{14}| + |\psi_{11}\rangle\langle\psi_{15}|) + \Omega_{ar}^{'}(t)(|\psi_{13}\rangle\langle\psi_9| + |\psi_{14}\rangle\langle\psi_{10}| + |\psi_{15}\rangle\langle\psi_{11}|), \\ h_2(t) = {} & \Omega_{b0}(t)(|\psi_3\rangle\langle\psi_1| + |\psi_7\rangle\langle\psi_5| + |\psi_{11}\rangle\langle\psi_9| + |\psi_{15}\rangle\langle\psi_{13}|) + \Omega_{b0}^{'}(t)(|\psi_1\rangle\langle\psi_3| + |\psi_5\rangle\langle\psi_7| + |\psi_9\rangle\langle\psi_{11}| + |\psi_{13}\rangle\langle\psi_{15}|) \\ & + \Omega_{br}(t)(|\psi_3\rangle\langle\psi_4| + |\psi_7\rangle\langle\psi_8| + |\psi_{11}\rangle\langle\psi_{12}|) + \Omega_{br}^{'}(t)(|\psi_4\rangle\langle\psi_3| + |\psi_8\rangle\langle\psi_7| + |\psi_{12}\rangle\langle\psi_{11}|), \\ h_3(t) = {} & \Omega_{ar}(t)|\psi_{12}\rangle\langle\psi_{16}| + \Omega_{ar}^{'}(t)|\psi_{16}\rangle\langle\psi_{12}|, \\ h_4(t) = {} & \Omega_{br}(t)|\psi_{15}\rangle\langle\psi_{16}| + \Omega_{br}^{'}(t)|\psi_{16}\rangle\langle\psi_{15}|, \end{aligned} \tag{A4}$$

and

$$\omega_1 = \Delta_a,\ \omega_2 = \Delta_b,\ \omega_3 = \Delta_a + V,\ \omega_4 = \Delta_b + V. \tag{A5}$$

According to Ref. [124], with the Hamiltonian in the form of Eq. (A4), one can derive the effective Hamiltonian as

$$H_{\text{eff}}(t) = \sum_{m,n=1}^{4} \frac{1}{\bar{\omega}_{mn}}[h_m^{\dagger}(t), h_n(t)]e^{i(\omega_m - \omega_n)t}, \tag{A6}$$

with

$$\frac{1}{\bar{\omega}_{mn}} = \frac{1}{2}\left(\frac{1}{\omega_m} + \frac{1}{\omega_n}\right), \tag{A7}$$

if condition

$$\max_{k,j}\{|\Omega_{kj}(t)|, |\Omega_{kj}^{'}(t)|\} \ll \min\{\Delta_a, \Delta_b, V\},\ \ (k = a,b;\ j = 0,r) \tag{A8}$$

is fulfilled. Moreover, by adding condition

$$\max_{k,j}\{|\Omega_{kj}(t)|, |\Omega_{kj}^{'}(t)|\} \ll |\Delta_a - \Delta_b|, \tag{A9}$$

the terms of $m \neq n$ in Eq. (A6) oscillate very quickly and can be omitted by considering the time average. Thus, Eq. (A6) can be further simplified as

$$\begin{aligned}
H_{\text{eff}}(t) = \sum_{n=1}^{4} \frac{1}{\omega_n}[h_n^{\dagger}(t), h_n(t)] &= \frac{\Omega_{a0}^2(t) - \Omega_{a0}^{'2}(t)}{\Delta_a}(|\psi_1\rangle\langle\psi_1| + |\psi_2\rangle\langle\psi_2| + |\psi_3\rangle\langle\psi_3| + |\psi_4\rangle\langle\psi_4|) \\
&+ \frac{\Omega_{ar}^2(t) - \Omega_{ar}^{'2}(t)}{\Delta_a}(|\psi_{13}\rangle\langle\psi_{13}| + |\psi_{14}\rangle\langle\psi_{14}| + |\psi_{15}\rangle\langle\psi_{15}|) + \frac{\Omega_{b0}^2(t) - \Omega_{b0}^{'2}(t)}{\Delta_b}(|\psi_1\rangle\langle\psi_1| + |\psi_5\rangle\langle\psi_5| + |\psi_9\rangle\langle\psi_9| \\
&+ |\psi_{13}\rangle\langle\psi_{13}|) + \frac{\Omega_{br}^2(t) - \Omega_{br}^{'2}(t)}{\Delta_b}(|\psi_4\rangle\langle\psi_4| + |\psi_8\rangle\langle\psi_8| + |\psi_{12}\rangle\langle\psi_{12}|) + \frac{\Omega_{a0}(t)\Omega_{ar}(t) - \Omega_{a0}^{'}(t)\Omega_{ar}^{'}(t)}{\Delta_a}(|\psi_1\rangle\langle\psi_{13}| \\
&+ |\psi_2\rangle\langle\psi_{14}| + |\psi_3\rangle\langle\psi_{15}| + \text{H.c.}) + \frac{\Omega_{b0}(t)\Omega_{br}(t) - \Omega_{b0}^{'}(t)\Omega_{br}^{'}(t)}{\Delta_b}(|\psi_1\rangle\langle\psi_4| + |\psi_5\rangle\langle\psi_8| + |\psi_9\rangle\langle\psi_{12}| + \text{H.c.}) \\
&+ \frac{\Omega_{a0}^{'2}(t) + \Omega_{ar}^{'2}(t) - \Omega_{a0}^2(t) - \Omega_{ar}^2(t)}{\Delta_a}(|\psi_9\rangle\langle\psi_9| + |\psi_{10}\rangle\langle\psi_{10}| + |\psi_{11}\rangle\langle\psi_{11}|) \\
&+ \frac{\Omega_{b0}^{'2}(t) + \Omega_{br}^{'2}(t) - \Omega_{b0}^2(t) - \Omega_{br}^2(t)}{\Delta_b}(|\psi_3\rangle\langle\psi_3| + |\psi_7\rangle\langle\psi_7| + |\psi_{11}\rangle\langle\psi_{11}|) + \frac{\Omega_{a0}^{'2}(t) - \Omega_{a0}^2(t)}{\Delta_a}|\psi_{12}\rangle\langle\psi_{12}| \\
&+ \frac{\Omega_{b0}^{'2}(t) - \Omega_{b0}^2(t)}{\Delta_b}|\psi_{15}\rangle\langle\psi_{15}| + \frac{\Omega_{ar}^2(t) - \Omega_{ar}^{'2}(t)}{\Delta_a + V}(|\psi_{16}\rangle\langle\psi_{16}| - |\psi_{12}\rangle\langle\psi_{12}|) \\
&+ \frac{\Omega_{br}^2(t) - \Omega_{br}^{'2}(t)}{\Delta_b + V}(|\psi_{16}\rangle\langle\psi_{16}| - |\psi_{15}\rangle\langle\psi_{15}|). \qquad \text{(A10)}
\end{aligned}$$

By substituting $\Omega_{k0}(t) = \Omega_{kr}(t) = \Omega_{k0}^{'}(t) = -\Omega_{kr}^{'}(t) = \Omega_k(t)$ $(k = a,b)$, Eq. (A10) can be simplified as

$$\begin{aligned}
H_{\text{eff}}(t) = &\frac{2\Omega_a^2(t)}{\Delta_a}(|\psi_1\rangle\langle\psi_{13}| + |\psi_{13}\rangle\langle\psi_1| + |\psi_2\rangle\langle\psi_{14}| + |\psi_{14}\rangle\langle\psi_2| + |\psi_3\rangle\langle\psi_{15}| + |\psi_{15}\rangle\langle\psi_3|) \\
&+ \frac{2\Omega_b^2(t)}{\Delta_b}(|\psi_1\rangle\langle\psi_4| + |\psi_4\rangle\langle\psi_1| + |\psi_5\rangle\langle\psi_8| + |\psi_8\rangle\langle\psi_5| + |\psi_9\rangle\langle\psi_{12}| + |\psi_{12}\rangle\langle\psi_9|). \qquad \text{(A11)}
\end{aligned}$$

Considering the initial state of the system is in $\{|\psi_1\rangle, |\psi_2\rangle, |\psi_5\rangle, |\psi_6\rangle\}$ (i.e, $\{|{+}{+}\rangle_{ab}, |{+}{-}\rangle_{ab}, |{-}{+}\rangle_{ab}, |{-}{-}\rangle_{ab}\}$) terms,

$$\frac{2\Omega_a^2(t)}{\Delta_a}(|\psi_3\rangle\langle\psi_{15}| + |\psi_{15}\rangle\langle\psi_3|) + \frac{2\Omega_b^2(t)}{\Delta_b}(|\psi_9\rangle\langle\psi_{12}| + |\psi_{12}\rangle\langle\psi_9|) \qquad \text{(A12)}$$

can be adiabatically removed from Eq. (A11). Thus, we can obtain Eq. (5).

[1] D. P. O'Leary, G. K. Brennen, and S. S. Bullock, Phys. Rev. A **74**, 032334 (2006).
[2] T. Li and F. G. Deng, Phys. Rev. A **94**, 062310 (2016).
[3] C.-P. Yang, Y. X. Liu, and F. Nori, Phys. Rev. A **81**, 062323 (2010).
[4] Y. Li, Phys. Rev. A **91**, 052328 (2015).
[5] C.-P. Yang, S.-I. Chu, and S. Han, Phys. Rev. A **70**, 044303 (2004).
[6] A. M. Childs, E. Farhi, and J. Preskill, Phys. Rev. A **65**, 012322 (2001).
[7] H. R. Wei and F. G. Deng, Opt. Express **22**, 593 (2014).
[8] Y. Cai, H. N. Le, and V. Scarani, Ann. Phys. (Berlin) **527**, 684 (2015).
[9] C.-P. Yang and S. Han, Phys. Rev. A **73**, 032317 (2006).
[10] P. W. Shor, in *1994 Proceedings of 35th Annual Symposium on Foundations of Computer Science* (IEEE, Washington, DC, 1994).
[11] L. K. Grover, Phys. Rev. Lett. **79**, 325 (1997).
[12] G. L. Long, Phys. Rev. A **64**, 022307 (2001).
[13] H. F. Hofmann, Phys. Rev. A **72**, 022329 (2005).
[14] R. M. Gingrich, C.-P. Williams, and N. J. Cerf, Phys. Rev. A **61**, 052313 (2000).
[15] G. A. Álvarez, E. P. Danieli, P. R. Levstein, and H. M. Pastawski, Phys. Rev. Lett. **101**, 120503 (2008).
[16] B. Paredes, F. Verstraete, and J. I. Cirac, Phys. Rev. Lett. **95**, 140501 (2005).
[17] J. Jing and L. A. Wu, Sci. Bull. **60**, 328 (2015).
[18] M. V. Berry, Proc. R. Soc. A **392**, 45 (1984).
[19] Y. Aharonov and J. Anandan, Phys. Rev. Lett. **58**, 1593 (1987).
[20] F. Wilczek and A. Zee, Phys. Rev. Lett. **52**, 2111 (1984).
[21] J. Anandan, Phys. Lett. A **133**, 171 (1988).
[22] P. Zanardi and M. Rasetti, Phys. Lett. A **264**, 94 (1999).
[23] L. A. Wu, P. Zanardi, and D. A. Lidar, Phys. Rev. Lett. **95**, 130501 (2005).
[24] L. X. Cen, Z. D. Wang, and S. J. Wang, Phys. Rev. A **74**, 032321 (2006).

[25] X. D. Zhang, Q. H. Zhang, and Z. D. Wang, Phys. Rev. A **74**, 034302 (2006).
[26] J. A. Jones, V. Vedral, A. Ekert, and G. Castagnoli, Nature (London) **403**, 869 (2000).
[27] A. A. Abdumalikov, Jr., J. M. Fink, K. Juliusson, M. Pechal, S. Berger, A. Wallraff, and S. Filipp, Nature (Landon) **496**, 482 (2013).
[28] S. Arroyo-Camejo, A. Lazariev, S. W. Hell, and G. Balasubramanian, Nat. Commun. **5**, 4870 (2014).
[29] B. B. Zhou, P. C. Jerger, V. O. Shkolnikov, F. J. Heremans, G. Burkard, and D. D. Awschalom, Phys. Rev. Lett. **119**, 140503 (2017).
[30] D. Kult, J. Åberg, and E. Sjöqvist, Phys. Rev. A **74**, 022106 (2006).
[31] L. Faoro, J. Siewert, and R. Fazio, Phys. Rev. Lett. **90**, 028301 (2003).
[32] L. M. Duan, J. I. Cirac, and P. Zoller, Science **292**, 1695 (2001).
[33] S. L. Zhu and Z. D. Wang, Phys. Rev. Lett. **91**, 187902 (2003).
[34] O. Oreshkov, T. A. Brun, and D. A. Lidar, Phys. Rev. Lett. **102**, 070502 (2009).
[35] V. N. Golovach, M. Borhani, and D. Loss, Phys. Rev. A **81**, 022315 (2010).
[36] J. T. Thomas, M. Lababidi, and M. Z. Tian, Phys. Rev. A **84**, 042335 (2011).
[37] P. Solinas, P. Zanardi, N. Zanghi, and F. Rossi, Phys. Rev. B **67**, 121307 (2003).
[38] G. F. Xu, J. Zhang, D. M. Tong, E. Sjöqvist, and L. C. Kwek, Phys. Rev. Lett. **109**, 170501 (2012).
[39] E. Sjöqvist, D. M. Tong, L. M. Andersson, B. Hessmo, M. Johansson, and K. Singh, New J. Phys. **14**, 103035 (2012).
[40] G. Feng, G. Xu, and G. Long, Phys. Rev. Lett. **110**, 190501 (2013).
[41] H. Li, Y. Liu, and G. Long, Sci. China Phys. Mech. **60**, 080311 (2017).
[42] J. Zhou, W. C. Yu, Y. M. Gao, and Z. Y. Xue, Opt. Express **23**, 14027 (2015).
[43] X. K. Song, H. Zhang, Q. Ai, J. Qiu, and F. G. Deng, New J. Phys. **18**, 023001 (2016).
[44] B. J. Liu, Z. H. Huang, Z. Y. Xue, and X. D. Zhang, Phys. Rev. A **95**, 062308 (2017).
[45] Z. Y. Xue, J. Zhou, Y. M. Chu, and Y. Hu, Phys. Rev. A **94**, 022331 (2016).
[46] Z. Y. Xue, J. Zhou, and Z. D. Wang, Phys. Rev. A **92**, 022320 (2015).
[47] Z. Y. Xue, F. L. Gu, Z. P. Hong, Z. H. Yang, D. W. Zhang, Y. Hu, and J. Q. You, Phys. Rev. Appl. **7**, 054022 (2017).
[48] J. Zhang, T. H. Kyaw, D. M. Tong, E. Sjövist, and L. C. Kwek, Sci. Rep. **5**, 18414 (2015).
[49] G. F. Xu, C. L. Liu, P. Z. Zhao, and D. M. Tong, Phys. Rev. A **92**, 052302 (2015).
[50] G. F. Xu, P. Z. Zhao, T. H. Xing, E. Sjöqvist, and D. M. Tong, Phys. Rev. A **95**, 032311 (2017).
[51] P. Z. Zhao, G. F. Xu, Q. M. Ding, E. Sjöqvist, and D. M. Tong, Phys. Rev. A **95**, 062310 (2017).
[52] Z. T. Liang, Y. X. Du, W. Huang, Z. Y. Xue, and H. Yan, Phys. Rev. A **89**, 062312 (2014).
[53] P. Z. Zhao, G. F. Xu, and D. M. Tong, Phys. Rev. A **94**, 062327 (2016).
[54] G. F. Xu, P. Z. Zhao, D. M. Tong, and E. Sjöqvist, Phys. Rev. A **95**, 052349 (2017).
[55] M. V. Berry, J. Phys. A **42**, 365303 (2009).
[56] X. Chen, I. Lizuain, A. Ruschhaupt, D. Guéry-Odelin, and J. G. Muga, Phys. Rev. Lett. **105**, 123003 (2010).
[57] A. del Campo, Phys. Rev. Lett. **111**, 100502 (2013).
[58] X. Chen, E. Torrontegui, and J. G. Muga, Phys. Rev. A **83**, 062116 (2011).
[59] A. del Campo, M. M. Rams, and W. H. Zurek, Phys. Rev. Lett. **109**, 115703 (2012).
[60] X. Chen, A. Ruschhaupt, S. Schmidt, A. del Campo, D. Guéry-Odelin, and J. G. Muga, Phys. Rev. Lett. **104**, 063002 (2010).
[61] E. Torrontegui, S. Ibánez, S. Martínez-Garaot, M. Modugno, A. del Campo, D. Guéry-Odelin, A. Ruschhaupt, X. Chen, and J. G. Muga, Adv. At. Mol. Opt. Phys. **62**, 117 (2013).
[62] J. G. Muga, X. Chen, A. Ruschhaupt, and D. Guéry-Odelin, J. Phys. B **42**, 241001 (2009).
[63] A. del Campo and M. G. Boshier, Sci. Rep. **2**, 648 (2012).
[64] S. Martínez-Garaot, E. Torrontegui, X. Chen, and J. G. Muga, Phys. Rev. A **89**, 053408 (2014).
[65] E. Torrontegui, S. Martínez-Garaot, and J. G. Muga, Phys. Rev. A **89**, 043408 (2014).
[66] H. Saberi, T. Opatrný, K. Mølmer, and A. del Campo, Phys. Rev. A **90**, 060301(R) (2014).
[67] B. T. Torosov, G. Della Valle, and S. Longhi, Phys. Rev. A **87**, 052502 (2013).
[68] B. T. Torosov, G. Della Valle, and S. Longhi, Phys. Rev. A **89**, 063412 (2014).
[69] S. Ibánez, X. Chen, E. Torrontegui, J. G. Muga, and A. Ruschhaupt, Phys. Rev. Lett. **109**, 100403 (2012).
[70] S. Ibánez, X. Chen, and J. G. Muga, Phys. Rev. A **87**, 043402 (2013).
[71] S. Ibánez and J. G. Muga, Phys. Rev. A **89**, 033403 (2014).
[72] S. Ibánez, Y. C. Li, X. Chen, and J. G. Muga, Phys. Rev. A **92**, 062136 (2015).
[73] X. K. Song, Q. Ai, J. Qiu, and F. G. Deng, Phys. Rev. A **93**, 052324 (2016).
[74] Y. H. Kang, Y. H. Chen, B. H. Huang, J. Song, and Y. Xia, Ann. Phys. (Berlin) **529**, 1700004 (2017).
[75] Y. H. Kang, Z. C. Shi, B. H. Huang, J. Song, and Y. Xia, Ann. Phys. (Berlin) **529**, 1700154 (2017).
[76] A. Baksic, H. Ribeiro, and A. A. Clerk, Phys. Rev. Lett. **116**, 230503 (2016).
[77] E. Torrontegui, S. Ibánez, X. Chen, A. Ruschhaupt, D. Guéry-Odelin, and J. G. Muga, Phys. Rev. A **83**, 013415 (2011).
[78] J. G. Muga, X. Chen, S. Ibánez, I. Lizuain, and A. Ruschhaupt, J. Phys. B **43**, 085509 (2010).
[79] E. Torrontegui, X. Chen, M. Modugno, A. Ruschhaupt, D. Guéry-Odelin, and J. G. Muga, Phys. Rev. A **85**, 033605 (2012).
[80] S. Masuda and K. Nakamura, Phys. Rev. A **84**, 043434 (2011).
[81] S. Masuda and S. A. Rice, J. Phys. Chem. A **119**, 3479 (2015).
[82] X. Chen and J. G. Muga, Phys. Rev. A **82**, 053403 (2010).
[83] X. Chen, E. Torrontegui, D. Stefanatos, J. S. Li, and J. G. Muga, Phys. Rev. A **84**, 043415 (2011).
[84] A. del Campo, Europhys. Lett. **96**, 60005 (2011).
[85] J. F. Schaff, X. L. Song, P. Vignolo, and G. Labeyrie, Phys. Rev. A **82**, 033430 (2010).
[86] Q. C. Wu, Y. H. Chen, B. H. Huang, Z. C. Shi, J. Song, and Y. Xia, Ann. Phys. (Berlin) **529**, 1700186 (2017).
[87] Y. H. Chen, Q. C. Wu, B. H. Huang, J. Song, Y. Xia, and S. B. Zheng, Ann. Phys. (Berlin) **530**, 1700247 (2018).
[88] X. Chen and J. G. Muga, Phys. Rev. A **86**, 033405 (2012).

[89] A. C. Santos, R. D. Silva, and M. S. Sarandy, Phys. Rev. A **93**, 012311 (2016).
[90] I. Hen, Phys. Rev. A **91**, 022309 (2015).
[91] Y. H. Kang, Y. H. Chen, Z. C. Shi, J. Song, and Y. Xia, Phys. Rev. A **94**, 052311 (2016).
[92] Y. H. Kang, Y. H. Chen, Z. C. Shi, B. H. Huang, J. Song, and Y. Xia, Phys. Rev. A **96**, 022304 (2017).
[93] S. Deffner, C. Jarzynski, and A. del Campo, Phys. Rev. X **4**, 021013 (2014).
[94] A. del Campo, Phys. Rev. A **84**, 031606(R) (2011).
[95] Y. H. Kang, Y. H. Chen, Q. C. Wu, B. H. Huang, Y. Xia, and J. Song, Sci. Rep. **6**, 30151 (2016).
[96] Y. C. Li, D. Martínez-Cercós, S. Martínez-Garaot, X. Chen, and J. G. Muga, Phys. Rev. A **97**, 013830 (2018).
[97] E. S. Kyoseva and N. V. Vitanov, Phys. Rev. A **73**, 023420 (2006).
[98] P. A. Ivanov, E. S. Kyoseva, and N. V. Vitanov, Phys. Rev. A **74**, 022323 (2006).
[99] P. A. Ivanov, B. T. Torosov, and N. V. Vitanov, Phys. Rev. A **75**, 012323 (2007).
[100] P. A. Ivanov and N. V. Vitanov, Phys. Rev. A **77**, 012335 (2008).
[101] N. V. Vitanov, Phys. Rev. A **85**, 032331 (2012).
[102] B. Rousseaux, S. Guerin, and N. V. Vitanov, Phys. Rev. A **87**, 032328 (2013).
[103] D. Daems, A. Ruschhaupt, D. Sugny, and S. Guérin, Phys. Rev. Lett. **111**, 050404 (2013).
[104] D. Sugny and C. Kontz, Phys. Rev. A **77**, 063420 (2008).
[105] L. Van-Damme, D. Schraft, G. T. Genov, D. Sugny, T. Halfmann, and S. Guérin, Phys. Rev. A **96**, 022309 (2017).
[106] A. P. Peirce, M. A. Dahleh, and H. Rabitz, Phys. Rev. A **37**, 4950 (1988).
[107] M. Saffman, T. G. Walker, and K. Mølmer, Rev. Mod. Phys. **82**, 2313 (2010).
[108] A. Browaeys, D. Barredo, and T. Lahaye, J. Phys. B **49**, 152001 (2016).
[109] M. Müller, I. Lesanovsky, H. Weimer, H. P. Büchler, and P. Zoller, Phys. Rev. Lett. **102**, 170502 (2009).
[110] H. Z. Wu, Z. B. Yang, and S. B. Zheng, Phys. Rev. A **82**, 034307 (2010).
[111] D. D. B. Rao and K. Mølmer, Phys. Rev. A **89**, 030301(R) (2014).
[112] T. Keating, R. L. Cook, A. M. Hankin, Y. Y. Jau, G. W. Biedermann, and I. H. Deutsch, Phys. Rev. A **91**, 012337 (2015).
[113] E. Brion, L. H. Pedersen, M. Saffman, and K. Mølmer, Phys. Rev. Lett. **100**, 110506 (2008).
[114] A. Gaëtan, Y. Miroshnychenko, T. Wilk, A. Chotia, M. Viteau, D. Comparat, P. Pillet, A. Browaeys, and P. Grangier, Nat. Phys. **5**, 115 (2009).
[115] J. Sanders, R. van Bijnen, E. Vredenbregt, and S. Kokkelmans, Phys. Rev. Lett. **112**, 163001 (2014).
[116] D. Jaksch, J. I. Cirac, P. Zoller, S. L. Rolston, R. Côté, and M. D. Lukin, Phys. Rev. Lett. **85**, 2208 (2000).
[117] D. Møller, L. B. Madsen, and K. Mølmer, Phys. Rev. Lett. **100**, 170504 (2008).
[118] M. M. Müller, M. Murphy, S. Montangero, T. Calarco, P. Grangier, and A. Browaeys, Phys. Rev. A **89**, 032334 (2014).
[119] M. Saffman, J. Phys. B **49**, 202001 (2016).
[120] S. L. Su, Y. Tian, H. Z. Shen, H. Zang, E. Liang, and S. Zhang, Phys. Rev. A **96**, 042335 (2017).
[121] X. Q. Shao, D. X. Li, Y. Q. Ji, J. H. Wu, and X. X. Yi, Phys. Rev. A **96**, 012328 (2017).
[122] H. Wu, X. R. Huang, C. S. Hu, Z. B. Yang, and S. B. Zheng, Phys. Rev. A **96**, 022321 (2017).
[123] T. Wilk, A. Gaëtan, C. Evellin, J. Wolters, Y. Miroshnychenko, P. Grangier, and A. Browaeys, Phys. Rev. Lett. **104**, 010502 (2010).
[124] D. F. V. James and J. Jerke, Can. J. Phys. **85**, 625 (2007).